Journal of
Water & Climate Change

IWA PUBLISHING

Journal of Water and Climate Change Vol 15 No 11, 5440 doi: 10.2166/wcc.2024.281

Changes in DOM and alum doses for two rivers of contrasting catchments after intense wildfires

Hiua Daraei [a,b,c,*], John Awad[a,d], Adam Leavesley[e], Mark Agnew[f], Eriita Jones[a,g], Matthew Gale[h], Kathy Cinque[IWA][i], Edoardo Bertone[b,c,j] and John van Leeuwen[a]

[a] Sustainable Infrastructure and Resource Management (SIRM), UniSA STEM, University of South Australia, Mawson Lakes, SA 5095, Australia
[b] School of Engineering and Built Environment, Griffith University, Gold Coast, QLD 4222, Australia
[c] Cities Research Institute, Griffith University, Gold Coast, QLD 4222, Australia
[d] CSIRO Environment, Waite Campus, Waite Rd., Urrbrae, SA 5064, Australia
[e] Parks and Conservation Service, Environment, Planning and Sustainable Development Directorate, Canberra, ACT 2601, Australia
[f] Kangaroo Island Landscape Board, Kingscote, SA 5223, Australia
[g] School of Earth and Planetary Sciences, Curtin University, Perth, WA 6845, Australia
[h] Fenner School of Environment & Society, Australian National University, Canberra, ACT 2601, Australia
[i] Melbourne Water, LaTrobe Street, Docklands, VIC 3008, Australia
[j] Australian Rivers Institute, Griffith University, Gold Coast, QLD 4222, Australia
*Corresponding author. E-mail: h.daraei@griffith.edu.au

HD, 0000-0002-1758-6568

ABSTRACT

The dynamics of dissolved organic matter (DOM) in two river waters were investigated after their catchments had been severely burnt in the 2019/20 Australian wildfires. Shortly after these wildfires, dissolved organic carbon (DOC) concentrations were recorded at high levels (~ 19 mg/L & 30 mg/L) and these became much lower (up to ~80% less) in the following winter when river flows had increased. Satellite imagery-based data indicated up to 95% of catchment areas burnt and up to ~50% subsequent vegetation recoveries after two years. Shifts in burn index values for the burnt areas coincided with DOC concentration variations. Specific colour of waters increased up to 40% as daily river flows increased, indicating higher input of humic content from the burnt catchments. Chlorophyll-a was detected at highest levels in waters soon after the fires when river flows were lowest. Enhanced alum doses were predicted using two feed-forward models; one based on DOC and turbidity data and the other based on UV@254nm, colour and turbidity. Doses predicted using the two models showed high correlations ($r > 0.9$) and were highest for waters directly after the fires. These models were developed for diverse source waters including those impacted by extreme climate events.

Key words: alum, DOC, DOM, remote sensing, wildfire

HIGHLIGHTS

- A two-year investigation offers comprehensive insights into post-wildfire water quality dynamics.
- Utilizing differenced normalized burn ratio (dNBR) data enhances understanding of catchment recovery post fire.
- Novel models for alum dosing are proposed to address fluctuating water quality.
- Integration of hydrology, remote sensing, and water treatment insights enriches understanding on wildfire impacts.
- Hydrology and water quality data highlight wildfire impacts on water resources.

GRAPHICAL ABSTRACT

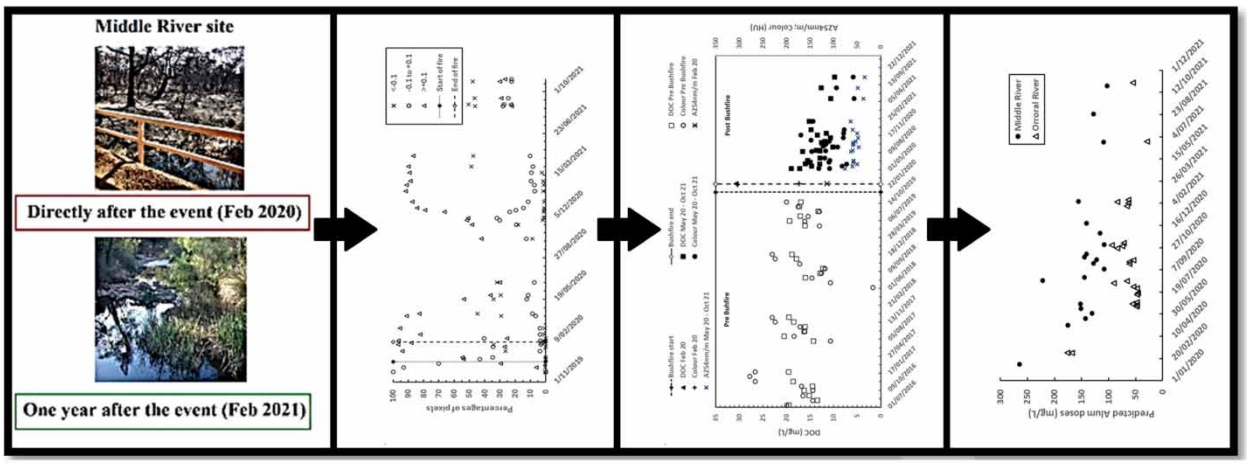

1. INTRODUCTION

Wildfires are a feature of the Australian landscape (Mannik *et al.* 2013; Nolan *et al.* 2021) that occur following extended periods of dry weather conditions and where fuel loads are high and moisture levels are low. Events such as the 2019–2020 Australian wildfires have been attributed to the effects of anthropogenic climate change driving increased temperature extremes with long-term warming trends (Nolan *et al.* 2021; van Oldenborgh *et al.* 2021). The impacts of large-scale wildfires or megafires can be severe, including widescale destruction of native fauna and flora, their habitats, loss of human life, and detrimental socioeconomic outcomes (Richards *et al.* 2020; Neris *et al.* 2021).

The impacts of wildfires on water quality have been widely reported, including investigations on the dynamics of turbidity, major ions, metals and heavy metals, polyaromatic hydrocarbons, nutrients (N and P), and organic matter quantified as total (TOC) or dissolved organic carbon (DOC) or as chemical oxygen demand (Quill *et al.* 2010; Sherson *et al.* 2015; Mansilha *et al.* 2019; Biswas *et al.* 2021; Johnston & Maher 2022). This also includes various studies that have applied fire severity and vegetation indices derived from satellite imagery data to assess the impacts of wildfires on water quality and streamflow dynamics. The normalized burn ratio (NBR) is a spectral index that provides an indication of photosynthetic biomass and soil and foliar moisture (Miller & Thode 2007; Chuvieco *et al.* 2020). Low (or negative) NBR values generally correspond to sparsely vegetated areas, such as bare ground or recent burns. The difference between the pre- and post-fire NBR products (dNBR) therefore provides an effective way to assess the degree of burn severity, and a general interpretation of dNBR values is given in Supplementary Table S1. Hogue & McCray (2018) utilized the dNBR index, derived from Landsat imagery, to map the impact of 159 fires across 153 burnt watersheds in the western United States. Their investigation aimed to discern post-fire water quality responses, revealing significant increases in nutrient, major-ion, and metal concentrations within the first 5 years after a fire event. Joehnk *et al.* (2020) also utilized dNBR to assess burn severity in the Upper Murray and the Mitta Mitta catchments, examining its ramifications on hydrology, sediment, nutrient transport, and subsequent water quality alterations in the receiving waters. Their findings highlighted severe implications for the water quality of River Murray and Lake Hume from the fires (Biswas *et al.* 2021).

Dissolved organic matter (DOM) is a ubiquitous component of fresh surface waters originating from natural and anthropogenic allochthonous sources in the catchment and by autochthonous production and degradation processes (Sachse *et al.* 2005; Young *et al.* 2005). Organic compounds that comprise DOM are derived from decomposition and biodegradation of plant and animal matter, synthetic organic matter, bacteria, and algae. These compounds vary highly in their characteristics including reactivity, molecular size, hydrophobicity/hydrophilicity, structural and functional groups, and elemental constituents (Mostofa *et al.* 2013; Wang *et al.* 2013). DOM is commonly measured as DOC and comprises humic substances (humic and fulvic acids) and non-humic compounds such as carbohydrates, proteins, amino acids, lipids, phenols, alcohols, organic acids, and sterols (Mostofa *et al.* 2013; Wang *et al.* 2013). DOM levels in fresh waters are influenced by a wide range

of factors, including amounts of organic matter (e.g. soil litter layers) present in catchments, soil sorption of DOM (Kaiser & Zech 1997), vegetation types and loadings, topography, seasonality, and climate conditions (Awad *et al.* 2015, 2017; Huang *et al.* 2015). Concentrations of DOC in fresh waters can range widely between different water sources (from <1 to $\gg 10$ mg/L) and vary highly among water sources depending on factors such as preceding rainfall intensities, vegetation types, soils, and topography within a catchment (Awad *et al.* 2015, 2016). DOM present in fresh waters can be significant based on it being a substrate for microbial growth fuelling microbial-based food webs (Kreutzweiser & Capell 2003; Young *et al.* 2005), transporting metals including heavy metals (Kaiser & Zech 1997), and at high concentrations, it can cause water to be highly coloured, attenuating light penetration that consequently limits photosynthetic activity in the water body (Mostofa *et al.* 2013). Conversely, DOM can attenuate the penetration of UV irradiance into the water body protecting aquatic organisms (Mostofa *et al.* 2013). High loadings of DOM can occur when catchments become inundated with surface water flows following heavy rainfalls, causing the transport of terrestrial particulate organic matter and DOM into rivers and streams (Mosley *et al.* 2021), potentially leading to elevated heterotrophic bacterial activity leading to oxygen depletion within the water body and then death of the aquatic organisms. Although negative impacts can occur on aquatic organisms, these events have also been noted as being of benefit in terms of supplying food and nutrients, increasing river productivity and benefiting waterbirds, native fish, and other aquatic organisms (DAWE 2023).

DOM present in drinking water sources can impart colour and comprise taste and odour compounds impacting on the aesthetic quality of water. Organic compounds that are recalcitrant to removal by conventional water treatment processes, i.e. coagulation and flocculation, can react with chlorine during disinfection, leading to halogenated disinfection by-products that can be of health concern (Teksoy *et al.* 2008; Golea *et al.* 2017), as well as being a substrate for microbial regrowth in drinking water distribution systems (Niquette *et al.* 2001). To minimize the formation of halogenated disinfection by-products in drinking waters, raw waters may be treated using enhanced coagulation, which practically maximizes the removal of DOM prior to chlorination, as required in the United States by the United States Environmental Protection Agency (USEPA) (Edzwald & Tobiason 1999) and applied elsewhere.

In this paper, we report the results of an investigation on the dynamics of DOM of two river waters from contrasting catchments following intense wildfires and the alum doses needed for enhanced coagulation in drinking water supply. These alum doses were derived using a model recently reported by Daraei *et al.* (2023a) where input data are DOC and turbidity. A further alum dose prediction model, which is based on input data of UV absorbance at 254 nm (UV@254 nm), true colour, and turbidity, is also described. These were developed for source waters with wide-ranging qualities including those impacted by the wildfires.

2. MATERIALS AND METHODS

2.1. River catchment descriptions

The Orroral River catchment (Figure 1) is located in the Namadgi National Park in the Australian Capital Territory (ACT). At lower elevations of the national park, the vegetation comprises tussock grasslands, bogs, woodlands, and forests; at medium elevations, mountain forests predominate, while at higher elevations, subalpine and alpine vegetation predominate. The Orroral River catchment is in an area zoned as conservation and recreational (ACT Government 2020). The Orroral River is perennial and flows into the Gudgenby River, part of the Murrumbidgee catchment within the Murray–Darling Basin. Waters from the Murrumbidgee River flow westwards supplying drinking water to towns and cities in proximity to this river, before discharging into the Murray River, which is a key water resource of South Australia, including for drinking water supply.

The Middle River catchment (Figure 1) has an area of ~14,500 ha located in the north of Kangaroo Island, South Australia. Prior to the fires, land uses in the catchment were dry land agriculture (mainly pasture, 50%), plantation forestry (pine and blue gums plantations, 12%), and conservation and natural environments (native vegetation, 38%) (DEWNR 2013). A land-use map for the Middle River catchment is shown in Supplementary Figure S1. The waters of the Middle River catchment flow into the Middle River Reservoir, which holds about 540 ML. The reservoir water, known for its high DOC concentrations and high colour levels, is treated using the Magnetic Ion Exchange (MIEX)® technology along with conventional treatment processes for drinking water supply.

2.2. Brief descriptions of 2019–2020 wildfires

Severe wildfires occurred in Australia during the 2019–2020 wildfire season affecting the ACT, New South Wales, Queensland, South Australia, Tasmania, Victoria, and Western Australia, with reported areas burnt of over 17 million hectares (ha)

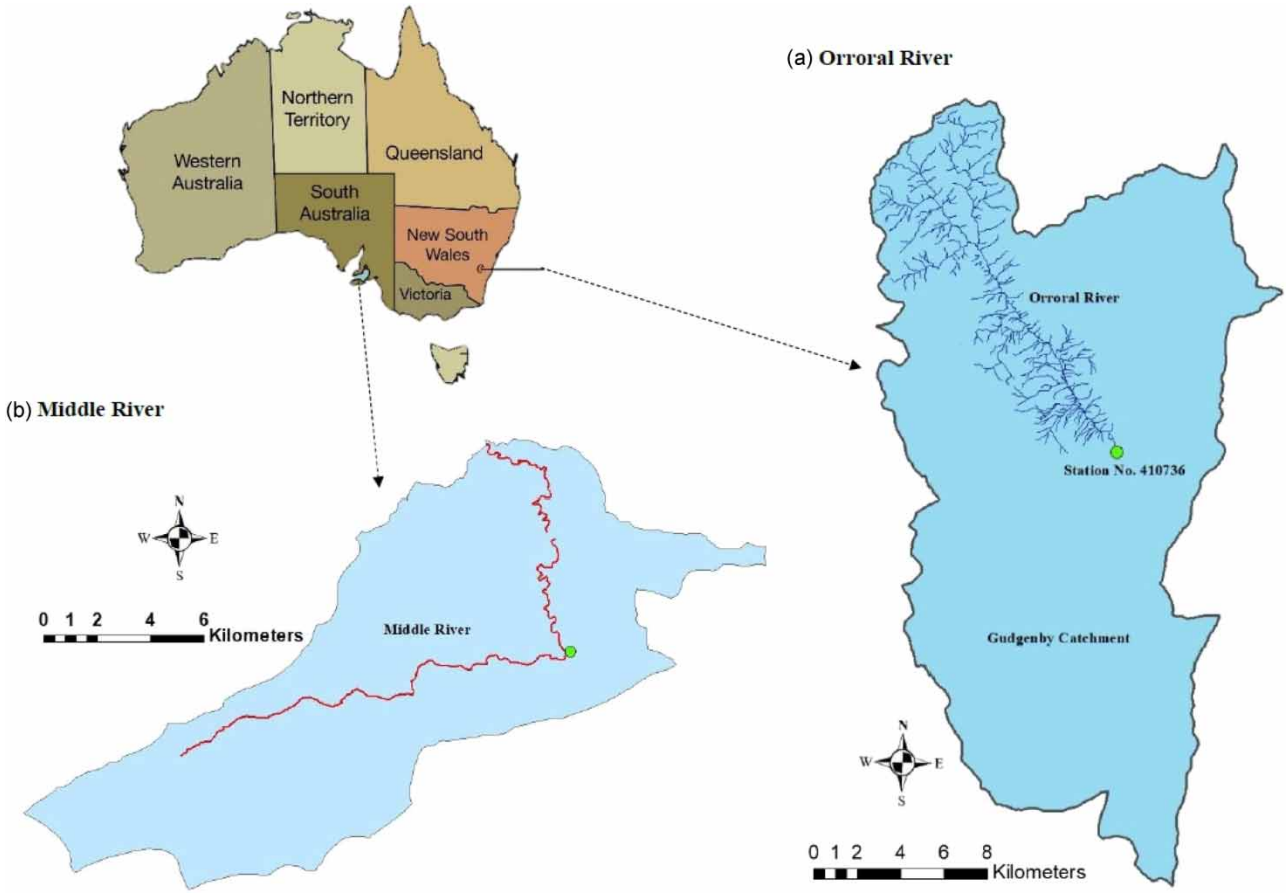

Figure 1 | Study area map and sampling points (●).

(Huff *et al.* 2020; Richards *et al.* 2020). The year 2019 was the warmest year on record in Australia up to that point, with record-low levels of rainfall over large areas of Australia. In most parts of tropical Western Australia and the Northern Territory, rainfalls had been well below average in the 2018–2019 wet season, resulting in very low soil moisture levels over most of the continent leading into December 2019. In December 2019, Australia experienced 11 days with a national area-averaged maximum of 40 °C or above, and on 18 December 2019, Australia experienced the hottest averaged day of 41.9 °C. In 2019, Australia had the highest December accumulated forest fire danger index (FFDI) since recording began in 1950 (BOM 2020).

The Orroral Valley fire started on 27 January 2020 and in the first 24 h, the fire had spread ~2,580 ha and then at 4,500–8,000 ha per day over the subsequent 3 days into the remote parts of the Namadgi National Park. Forest fuel loads were exceptionally dry and approximately 78% (over 82,700 ha) of the Namadgi National Park was burnt during the fire (ACT Government 2020). Kangaroo Island has a total area of over 440,000 hectares of which approximately a third is a nature reserve. During the 2019/2020 wildfires, about 38% of the island was burnt, of which 83% was burnt at high to very high severity (DCCEEW 2022). The Middle River catchment was extensively burnt in the summer fires.

2.3. Water sampling and locations

The Orroral River water sampling site (35.66512S, 148.98929E) is located in the Namadgi National Park, Canberra, and the Middle River site (35.7349S, 137.1032E) is located on Kangaroo Island South Australia. Water samples were collected from the Orroral River as grab samples and from the Middle River, predominantly using a composite sampler. The composite sampler was programmed to pump 500 mL of uniform increments of flow into an unrefrigerated container. The water samples were collected in PET bottles, transported chilled to the laboratory, and stored at ~4 °C until analyses were performed. After the fires, sampling was undertaken from February 2020 through to November 2021, when access to sampling sites

of the burnt catchments was logistically feasible. In February and March 2020, soon after the fires had occurred, grab samples were collected from both sites.

2.4. Water quality analyses

Water samples were filtered using 0.45 μm polyether-sulfone membrane filters (Sartorius, Germany) for DOC, ultraviolet–visible (UV–Vis), and colour analyses. DOC analysis was performed using either a TOC analyser (O I Analytical, Aurora 1030 – wet oxidation) for samples collected prior to the Kangaroo Island wildfires (by the Australian Water Quality Centre, SA Water Corporation, a NATA registered laboratory) and using a Sievers InnovOx Laboratory TOC analyser (GE Instruments, USA) at the University of South Australia for samples collected after the wildfires had occurred. For DOC analyses of water samples, a series of DOC standards were prepared from potassium hydrogen phthalate stock solutions (100 mg C/L) and analysed with the water samples. UV light absorbance at 254 nm (A254) was determined using a UV–Vis spectrophotometer, Agilent Technologies Cary 60, for samples collected prior to the Kangaroo Island wildfires at the Australian Water Quality Centre, SA Water Corporation, and by Model UV-120 (Miostech, Australia) equipped with a 1 cm quartz cuvette for grab samples collected after the wildfires had occurred. Sample measurements were taken after the instrument was set to zero with high-purity Milli Q water high-purity Milli Q water in the same cuvette. The colour of the samples was measured at 456 nm using a 5 cm glass cuvette. A 50 Hazen unit (HU) colour standard (platinum-cobalt) was used for calibration after the instrument was set to zero with high-purity Milli Q water, high-purity Milli Q water, as reported by Bennett & Drikas (1993).

Turbidity (FNU) was measured using a YSI EXO2 multi-parameter sonde with turbidity probe (YSI, Yellowsprings, USA) or otherwise by a benchtop turbidity meter (Model 2100n, Hach, USA). The YSI EXO2 turbidity probe was calibrated according to the manufacturer's instructions, using standard turbidity solutions (<0.5, 100, and 500 NTU, analytical reagent (AR) grade, Rowe Scientific/Aim Scientific, South Australia). The Hach turbidity meter was calibrated using Hach 2659505 StablCal Turbidity standards (<0.1, 20, 200, 1,000, and 4,000 NTU), also according to the manufacturer's instructions. The turbidity of water samples and standards were cross-checked between the YSI EXO2 turbidity probe (FNU) and the Hach turbidimeter (NTU) and calibrated to ensure the readings were directly comparable.

The total dissolved solids (TDS) parameter was determined from the electrical conductivity of water measured using an EXO EC/temperature probe (Xylem Australia) after calibration using a 1413 micro Siemens standard solution. In this study, the coefficient of variation (CV) values for analyses of water quality parameters were as follows: for A254 nm/m 1.3%, true colour (HU) 8.0%, DOC (mg/L) 3.4%, turbidity (FNU) 0.85%, and TDS (mg/L) 0.1%. Chlorophyll a (Chl a) was measured using a YSI EXO2 Sonde (Xylem, USA) multi-meter equipped with a Chl a probe (excitation/emission paired wavelengths (ex/em) of 470 [±15]/685 [±20] nm, EXO Chl a probe) along with other probes (including pH, turbidity, temperature, and conductivity) as previously described (Daraei *et al.* 2023b). The Chl a probe was calibrated using a standard Rhodamine B solution, according to the manufacturer's instructions.

2.5. Estimation of catchment burn severity and vegetation recovery

Burn severity and vegetation recovery in the Orroral and Middle River catchments were assessed using Sentinel-2A/B MultiSpectral Instrument (MSI) satellite data, which were acquired via Digital Earth Australia's (DEA) imagery collection (Krause *et al.* 2021; Lewis *et al.* 2017). Terrain-corrected bottom-of-atmosphere reflectance products with nadir view angle were used to reduce differences between acquisitions caused by varying sun and view angles (Li *et al.* 2010, 2012). The products are accessible via the THREDDS server maintained by the DEA program as part of the National Computational Infrastructure (NCI). The data are pre-tiled and stored in 100 × 100 km tiles in a UTM/WGS84 (EPSG:32753) projection at 20-m resolution in GeoTIFF format. Invalid reflectance pixels, caused by cloud cover or terrain effects, were indicated by the DEA Function of Mask product, and excluded from analyses. Cloud-free imagery acquisitions were selected to coincide with water sampling dates, withstanding unavoidable differences caused by the 6-day satellite revisit frequency. The extent and severity of the burnt areas within the catchments were assessed using the NBR. The NBR is calculated as the normalized difference between the near-infrared (NIR) and shortwave infrared (SWIR) reflectance (Escuin *et al.* 2008), which for Sentinel-2 is given by Equation (1):

$$\mathrm{NBR} = \frac{\mathrm{b8} - \mathrm{b12}}{\mathrm{b8} + \mathrm{b12}} \tag{1}$$

where b8 is the NIR band (centred at 842 nm) and b12 is the SWIR2 band (centred at 2,190 nm).

The NBR images were produced for each acquisition close to a water sampling date, where possible, and geographic information system (GIS) boundaries of the water catchments were used to restrict the analysis to values within the catchments. Imagery dates for the Orroral River and Middle River catchments are given in Supplementary Table S2. Post-fire vegetation recovery within the catchments was implied by the recovery of NBR towards pre-fire values. This was indicated by examining the shift through time in the ratios of the burnt, unburnt, and regrowth pixel areas.

2.6. Alum dose determinations

Model-based alum dose determinations were made using a recently developed model that has raw water DOC concentration and turbidity as input variables (Daraei *et al.* 2023a) and a modified version of the *mEnCo*© model that is based on UV absorbance at 254 nm/cm, true colour measured at 456 nm, and turbidity. The models were developed using data acquired from jar testing of multiple water samples with diverse water quality characteristics, collected across Australia (Daraei *et al.* 2023a). These models comprise mathematical equations that relate the water quality parameters (DOC and turbidity; UV@254 nm/cm with or without colour (at 456 nm), and turbidity) with alum dose. Alum doses determined using the DOC model were based on achieving targeted removals of the coagulable fraction of DOM, measured as 89% of coagulable DOC, for waters of catchments where major wildfires have occurred, as previously reported by Daraei *et al.* (2023a). For the wide range of surface waters investigated by Daraei *et al.* (2023a), the average coagulable DOC was found to be 57.3% (SD $\pm$ 13.3) of the total DOC measured. For alum dose determinations using the DOC model and targeting 89% removal of the coagulable DOC, the model is as follows:

$$\text{Alum(mg/L)} = -\ln(0.11) \times C_{\text{DOC, alum}} \tag{2}$$

where $C_{\text{DOC, alum}} = f \times \text{DOC}^g$, and f and g are coefficients detailed by Daraei *et al.* (2023a).

The *mEnCo*© model's (van Leeuwen *et al.* 2005, 2009) original algorithms (for alum dosing) were updated using previously acquired data (van Leeuwen *et al.* 2023) along with further data acquired from jar testing of surface waters from catchments that had experienced extreme climate events (tropical cyclone and wildfires) reported by Daraei *et al.* (2023a) (see Supplementary Figure S2). In this modified model's application, the alum dose (as $Al_2(SO_4)_3{:}18H_2O$ (mg/L)) is the lower of two values determined using two separate algorithms. One value is based on raw water UV@254 nm/cm data only, while the second is based on UV@254 nm/cm and colour (measured at 456 nm). The rationale for having both options is to enable dose prediction with or without colour data being available, with UV@254 nm/cm data. The lower dose selection is based on minimizing alum dose usage while aiming to achieve target water quality. The corresponding algorithms are as follows:

$$\text{Alum(mg/L)} = a \times \text{UV@254 nm/cm} + b \tag{3}$$

$$\text{Alum(mg/L)} = c \times \text{UV@254 nm/cm} \times \log_{10}(\text{colour} \times 10) + d \tag{4}$$

where, in this study, $a = 226.5$, $b = 12.7$, $c = 71.5$, and $d = 15$ for raw waters with UV@254 nm/cm > 0.2.

The correlation coefficients, r, between the enhanced alum doses (determined by jar tests) and the corresponding model fitted doses using the aforementioned Equations (2)–(4) are 0.9663, 0.9858, and 0.9745, respectively. Enhanced alum doses were based on $\Delta\text{DOC}/\Delta\text{Alum} = -0.015$ mg/mg, as previously described (van Leeuwen *et al.* 2005; Daraei *et al.* 2023a). These models were developed for predictive estimation of coagulant doses where, in application at water treatment plants, verification of dose suitability by jar testing is recommended. In this study, model-based alum doses were considered for comparative assessment of coagulant (alum) requirements for water treatment of river waters from local and contrasting catchments impacted by extreme wildfire events and, subsequently, with catchment recoveries. Direct comparisons of the model-determined alum doses with coagulant use at operational drinking water treatment plants were not possible. This was due to their large distances downstream (and with inflows from other catchments) from the sampling point in the case of the Orroral River. In the case of the Middle River, this river flows into a storage reservoir, which then provides source water to a MIEX treatment plant.

2.7. Statistical analyses

The fitting of linear regression lines, determinations of linear equations, coefficients of determinations, and correlation coefficients, reported at 95% confidence were acquired using the Data Analysis add-in package function in Microsoft Excel.

3. RESULTS AND DISCUSSION

The extent of fire damage to the catchments of the Middle and Orroral Rivers from the summer wildfires of 2019–2020 and vegetation regrowth were investigated using Sentinel-2A/B MultiSpectral Instrument (MSI) satellite data. Frequency histograms of dNBR data of the Middle River and Orroral River catchments were generated during the first year after the fires (detailed in Supplementary Table S2) and shown in Figure 2.

Three categories (burnt, $>+0.1$; unburnt, -0.1 to $+0.1$; revegetated, <-0.1) areas (as pixels) of Sentinel-2 dNBR data are shown in Figure 3. Higher percentages of pixels of dNBR < 0 are associated with the regeneration of vegetation leaf area (Massetti *et al.* 2019), soil and foliar moisture (Miller & Thode 2007; Chuvieco *et al.* 2020).

Figure 3 shows high percentages of burnt catchment areas (as imagery pixels) directly after the fires for both catchments. Over the following 2 years, the Middle River catchment showed a cyclic pattern where these percentages reduced, along with vegetation regrowth, to ~40 to 50% in the late autumn to spring seasons and then increased again in the following summer (Figure 3(a)). The increases in the summer of 2020/2021 are likely a result of the Middle River catchment containing extensive pastures, the curing of grasses, and their reductions as feed for livestock. In the case of the Orroral River catchment, there was a consistent decline from the very high initial percentages of burnt areas directly after the wildfires, over the 2 years of

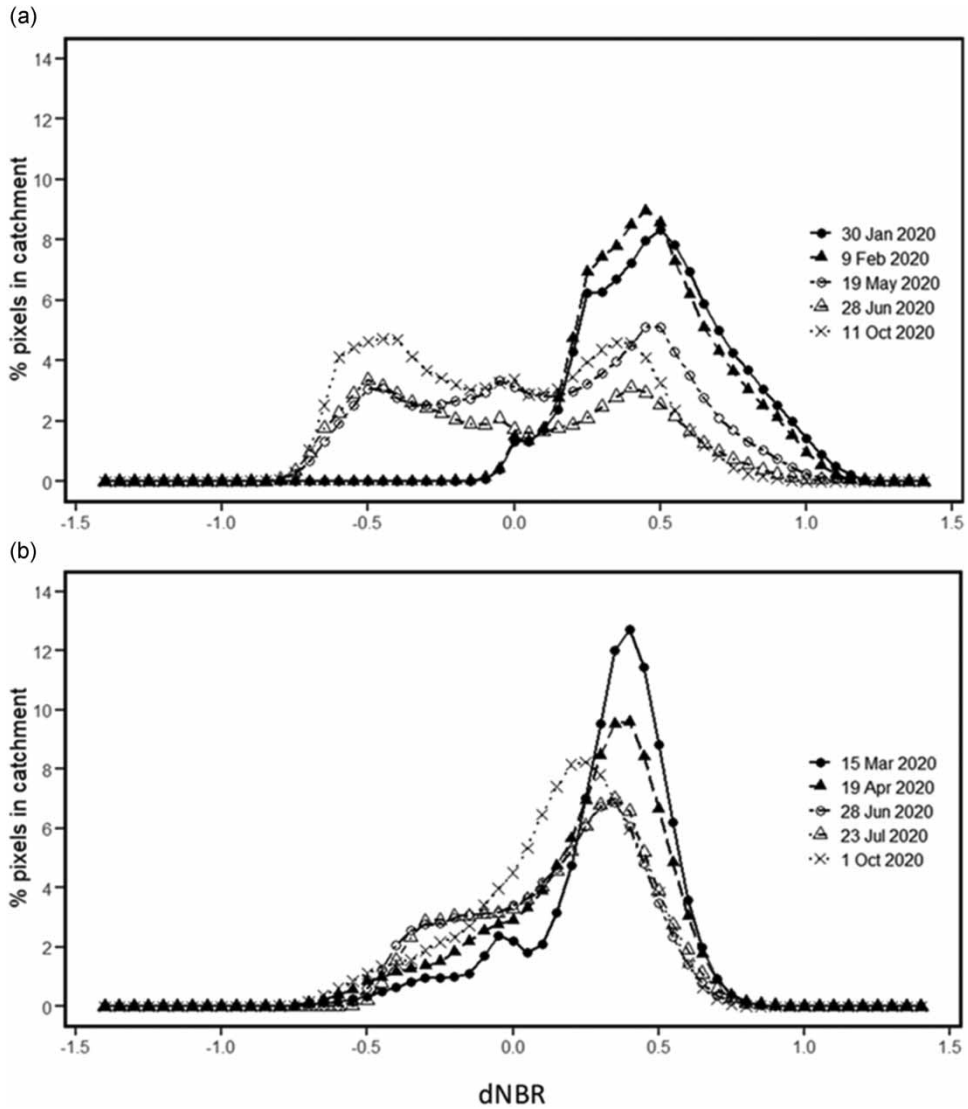

Figure 2 | Sentinel-2 dNBR frequency histograms of (a) Middle River and (b) Orroral River catchments for 2020.

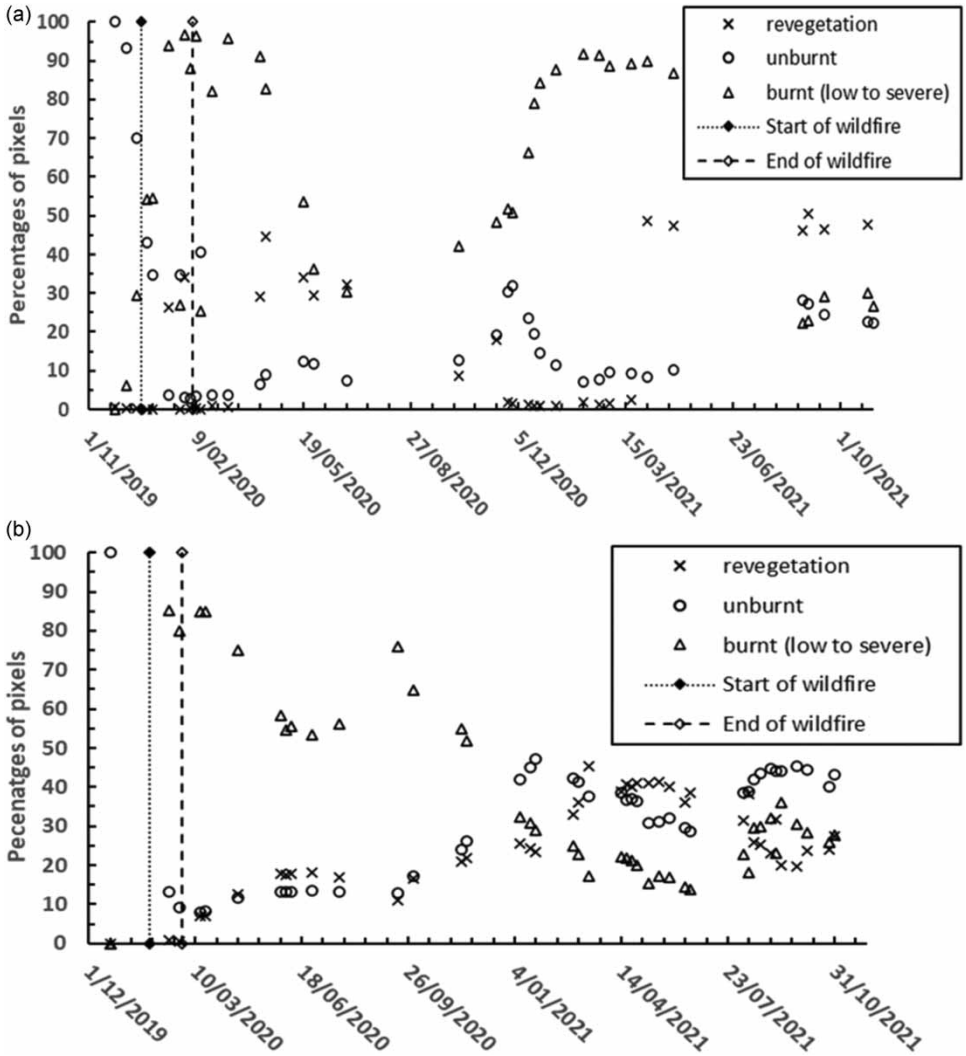

Figure 3 | Sentinel-2 dNBR data grouped into categories for (a) Middle River and (b) Orroral River catchments from late 2019 to the end of 2021 (*Note*: Burnt (low to severe): $>+0.1$; unburnt: -0.1 to $+0.1$; regrowth: <-0.1, see also Key & Benson (2006)).

monitoring (Figure 3(b)). In both catchments, revegetation is indicated from dNBR data, but this occurred more consistently in the Orroral catchment where vegetation is predominantly of native forests that are less susceptible to seasonality (than pastures). In a study of the Orroral Valley fire, reported by Gale *et al.* (2022), dNBR data demonstrated strong agreement with scorched and fire-consumed understory and canopy vegetation (Gale *et al.* 2022). The slower % increases of pixels of dNBR < -0.1 for the Orroral River catchment in the first year after the wildfire, compared with the Middle River catchment, may be attributed to slower regeneration of the dominant subalpine and woodland eucalypt-dominated forest types (Caccamo *et al.* 2015; Gibson & Hislop 2022). By comparison, the greater cover of grasslands in the Middle River catchment may have led to a more rapid increase of % pixels in dNBR < -0.1 in the following autumn to winter, since grasses quickly restore their greenness and photosynthetic capacity after fire and rainfalls (Lu *et al.* 2016; Fornacca *et al.* 2018). Nonetheless, the rapid increase in % pixels of dNBR < -0.1 in the Middle River catchment again declined to very low percentages in the following summer and early autumn (2020/2021).

Detrimental impacts from catchment wildfires on surface water qualities can be a major concern and these have been commonly reported (e.g. Sherson *et al.* 2015; Biswas *et al.* 2021; Neris *et al.* 2021; Johnston & Maher 2022). For the two rivers studied, the peak of DOM concentrations were observed soon after the end of fire events (February 2020 for the Middle River and March 2020 for the Orroral River, see Figure 4). In the case of the Orroral River, a storm event occurred in its catchment in January 2020 that led to short-term high flows (up to ~6.25 m^3/s or ~540 MLD, Supplementary Figure S3, with monthly

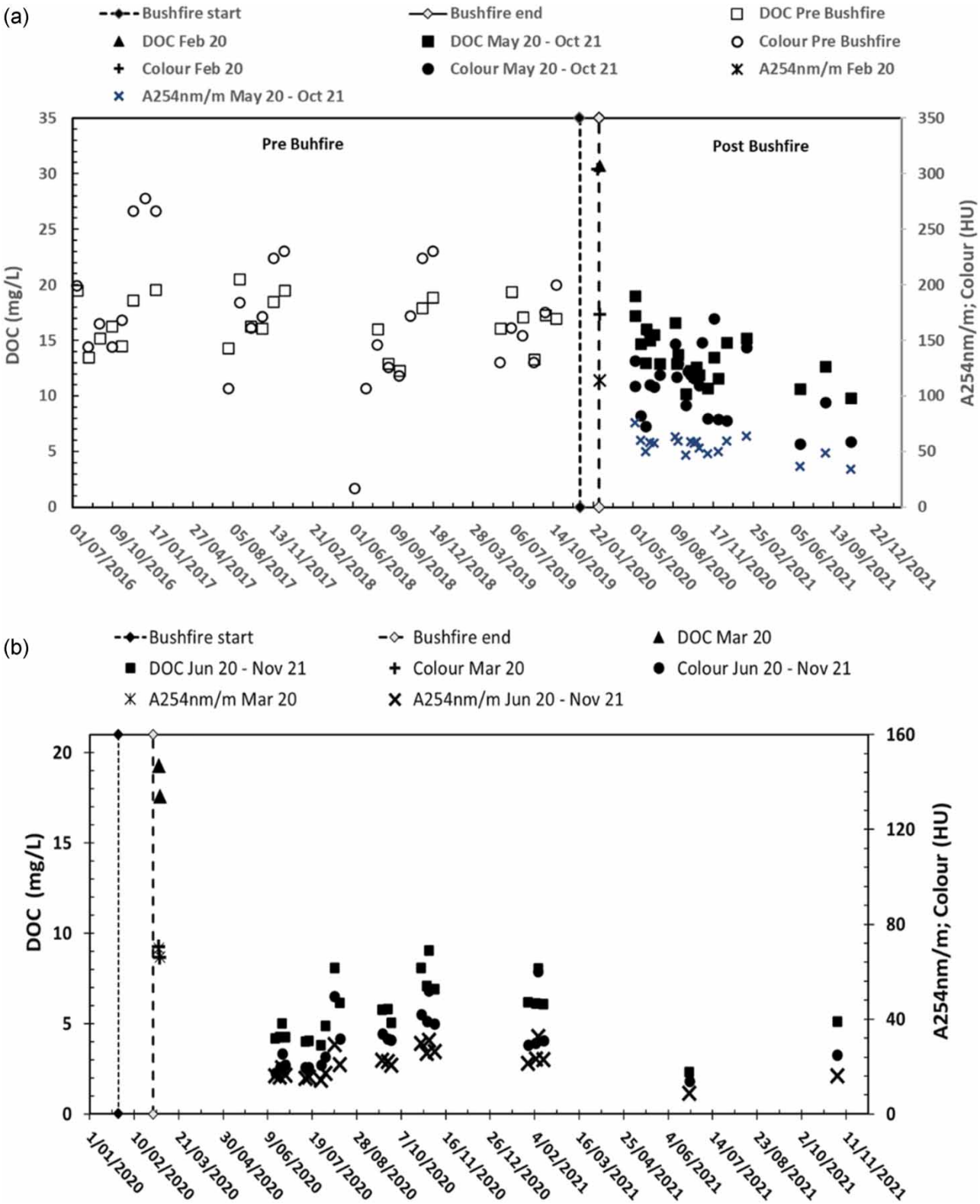

Figure 4 | DOC, A254 nm/m, and colour of (a) Middle River and (b) Orroral River before the 2019/2020 wildfires (where available) and afterwards to November 2021.

rainfall shown in Supplementary Figure S4). Also, there had been a short-duration high flow event in the Middle River catchment in early February 2020 at the end of the wildfire event, which mobilized large volumes of ash and silt. However, this flow event was not recorded because the monitoring site and equipment had been destroyed by the fire (subsequently replaced by a mobile unit). Despite these summer flow events, the DOC concentrations measured soon afterwards were much higher than the concentrations of samples collected subsequently, from late autumn/early winter to the spring of 2020 (Figure 4). Johnston & Maher (2022) reported on the concentrations and characters of dissolved organics during the first-flush period after a wildfire event had occurred and subsequently in the Macleay River, Australia. They found that initial hydrograph peaks during the post-fire period displayed a distinct increase in DOC concentration compared with the pre-fire condition, as similarly found in the present study for the Middle River (Figure 4). In this study, from the end of autumn, DOC and UV@254 nm/cm levels were much lower than directly after the fires had occurred. Declines in DOC and A254 nm/m occurred in Middle River waters from May 2020 onwards (Figure 4(a)) whereas for the Orroral River waters, DOC, A254 nm/m, and colour levels were relatively consistent from June 2020 to November 2021 (Figure 4(b)). Declines in the concentrations of DOM in the Orroral River waters from the high level recorded soon after the wildfire had occurred coincided with dNBR data that indicated steady vegetation regrowth (Figure 3(b)). By contrast, the declines in DOM levels in the Middle River waters occurred along with cyclic vegetation regrowth after the wildfire (Figure 3(a)), indicating factors other than regrowth impacting DOM concentrations. Highly elevated levels of DOM in the river waters soon after the wildfires had occurred may have resulted from concentration effects through high evaporation rates caused by the extreme temperatures from the wildfires, destruction of riverine vegetation increasing exposure of river waters to direct sunlight and winds, and subsequent higher summer temperatures. A high river flow event was recorded for the Orroral River in January 2020, and in early March, DOC levels were more than twice that of water samples subsequently collected.

The elevated levels of DOM might have occurred also through the high growth of cyanobacteria immediately after the wildfires and summer rainfalls that resulted in inflows to the rivers with high levels of nutrients from the burnt catchments. Chlorophyll a levels in the water samples collected from both rivers soon after the wildfires and following summer rainfalls were higher than levels subsequently measured from late autumn to the following summer (see Figure 5). Elevated levels of nutrient transport into waterways following heavy rainfalls post wildfires from burnt catchments have been reported by Sherson *et al.* (2015) and Biswas *et al.* (2021). Neris *et al.* (2021) and Biswas *et al.* (2021) also noted potential impacts on algal dynamics and bloom growth from the transport of nutrient-laden ash from burnt catchments into receiving waters.

Turbidity and TDS levels were measured over the study period, and data acquired are detailed in Supplementary Figure S5. Turbidity levels of the Middle River tended to be higher than those of the Orroral River but were very low in comparison to the high levels (up to 4,200 NTU) reported by Biswas *et al.* (2021) for the Jingellic site on the Murray River. Turbidity and river

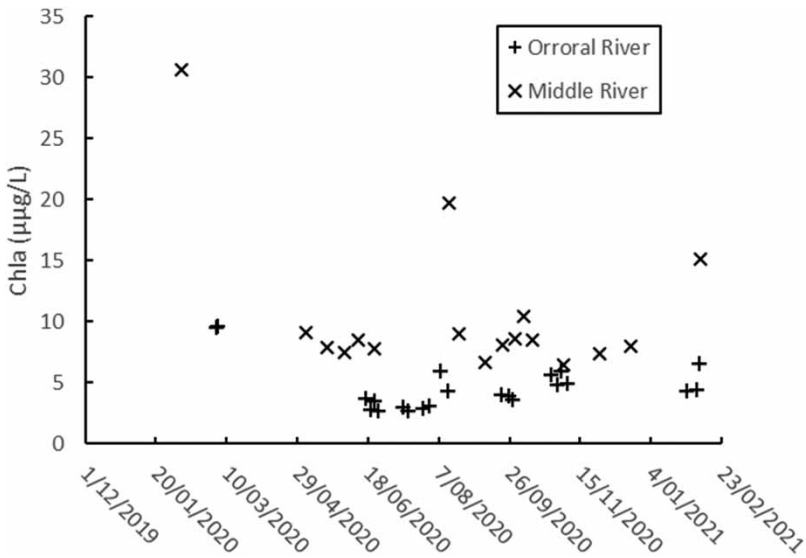

Figure 5 | Chlorophyll a levels of Middle and Orroral River water samples collected during the first year after the 2019/2020 wildfires.

flow rate data acquired in this study indicate that turbidity levels became generally higher as river flow rates increased (Supplementary Figure S6). However, other factors such as the soil and vegetation types and land practices of the catchment where rainfalls occurred would have likely been influential. The TDS levels of Middle River waters were much higher than those of the Orroral River, but in both cases, levels were generally higher when river flow rates were lower (Supplementary Figure S7). This indicates that elevated evaporation rates may have contributed to some extent to the very high concentrations of DOM found in the river waters in the summer of 2020. Alternatively, elevated DOM and TDS may have been the result of the summer rainfalls and associated catchment inflows.

Trends in DOC, colour, A254 nm/m, and turbidity with river flows (m^3/s) following the wildfires to February 2021 are shown in Figure 6(a) for the Middle River and Figure 6(b) for the Orroral River. At very low daily flows in February and March 2020, concentrations of DOC, A254 nm/m, and colour were highest. These initial high levels decreased as river flows increased in late autumn and winter, and then subsequently varied, either increasing (Middle River: colour; Orroral River: DOC, A254 nm/m, colour, and turbidity; $p < 0.05$) or otherwise no significant trends were found. Specific ultraviolet absorbance (SUVA) and specific colour (SpCol) levels in relation to river flows are shown in Figure 7(a) for the Middle River and Figure 7(b) for the Orroral River. For both rivers, there was little change in SUVA over the period monitored, while SpCol showed significant increases as flows increased ($p < 0.05$), indicating inputs of humic compounds that are characteristic of high colour into the two rivers from catchment sources.

The reductions in DOC, A254 nm/m, and colour from the initial high levels recorded following the fires may have been due to catchment surface and subsurface water inflows to the rivers, and assuming these were lower in concentrations, then diluting these parameters in the river waters, along with their transport downstream. Reductions from the high levels of DOM recorded may also have been due to their degradation by microbial processes. Generally, higher catchment flows result in greater transport of particulate matter and DOM derived from catchment vegetation into waterways (Dalva & Moore 1991; Murshed *et al.* 2014; Ke *et al.* 2022) and increases in these parameters following the initial decline are consistent with that characteristic. In a modelling study analysing the water quality impacts of extreme events on an Australian reservoir, a higher risk of poor water quality was predicted for a 'rain after fire' compared with a fire-only scenario (Bertone *et al.* 2016, 2018), thus highlighting the impact of flow-induced DOM transport from the catchment. Sherson *et al.* (2015) studied nutrient dynamics in a stream following a wildfire (Las Conchas wildfire in June 2011 that burnt ~36% of the contributing watershed) and during several precipitation events. They found significant increases occurred in dissolved NO_3-N (>6 times the background levels), dissolved phosphate (>100 times the background levels), specific conductance (>5 times the background levels), and turbidity (>100 times the background levels). These increases occurred along with substantial lowering in dissolved oxygen (<4 mg/L) and pH (<6.5). Their study highlighted the rapid rates of change in water quality during flow events following wildfires, lasting for a short duration.

Both rivers flow into surface water resources that are utilized for drinking water supply (Section 2.1), and a comparison of alum dose requirements for enhanced coagulation for the two river waters post the fires was investigated. Alum dose determinations were made using a model recently reported by Daraei *et al.* (2023a) that is based on DOC and turbidity data as the input variables. Data applied to develop the model included the results from jar testing of the water samples collected soon after the fires had occurred, i.e. 273 mg/L for the Middle River and 200 mg/L for the Orroral River (Daraei *et al.* 2023b). Model-determined alum doses are initially very high and subsequently are much lower over time and with increased river flows (Figure 8). On one occasion (14 August 2020), a recorded relatively high turbidity (144 NTU) for a Middle River water sample elevated the model-determined alum dose to over 200 mg/L. In the case of the Orroral River, after the initial high alum doses for water samples collected soon after the fire, model-determined doses became much lower where flow rates were less than 5 m^3/s, and then generally increased as the river flow rates increased to ~40 m^3/s (Figure 8(b)), tracking the increases in DOC concentrations (Figure 8(b)).

The data reported by Daraei *et al.* (2023a) were used to modify (Section 2.6) an established coagulant dose prediction model, *mEnCo*© (van Leeuwen *et al.* 2005, 2009) that has UV@254 nm/cm, colour (HU), and turbidity as input data. This was done to extend the alum dose prediction range of this model for waters with DOC concentrations from the current ~14 to 30 mg/L (or to ~1.15 UV@254 nm/cm). Comparisons of alum doses determined using the two models for the two waters are shown in Figure 9, and these doses are generally similar for the same water sample when the models were set to achieve enhanced coagulation. These models have potential benefits in terms of providing dose predictions based on the different water quality parameters, which can be readily measured at a water treatment plant or at an associated analytical laboratory

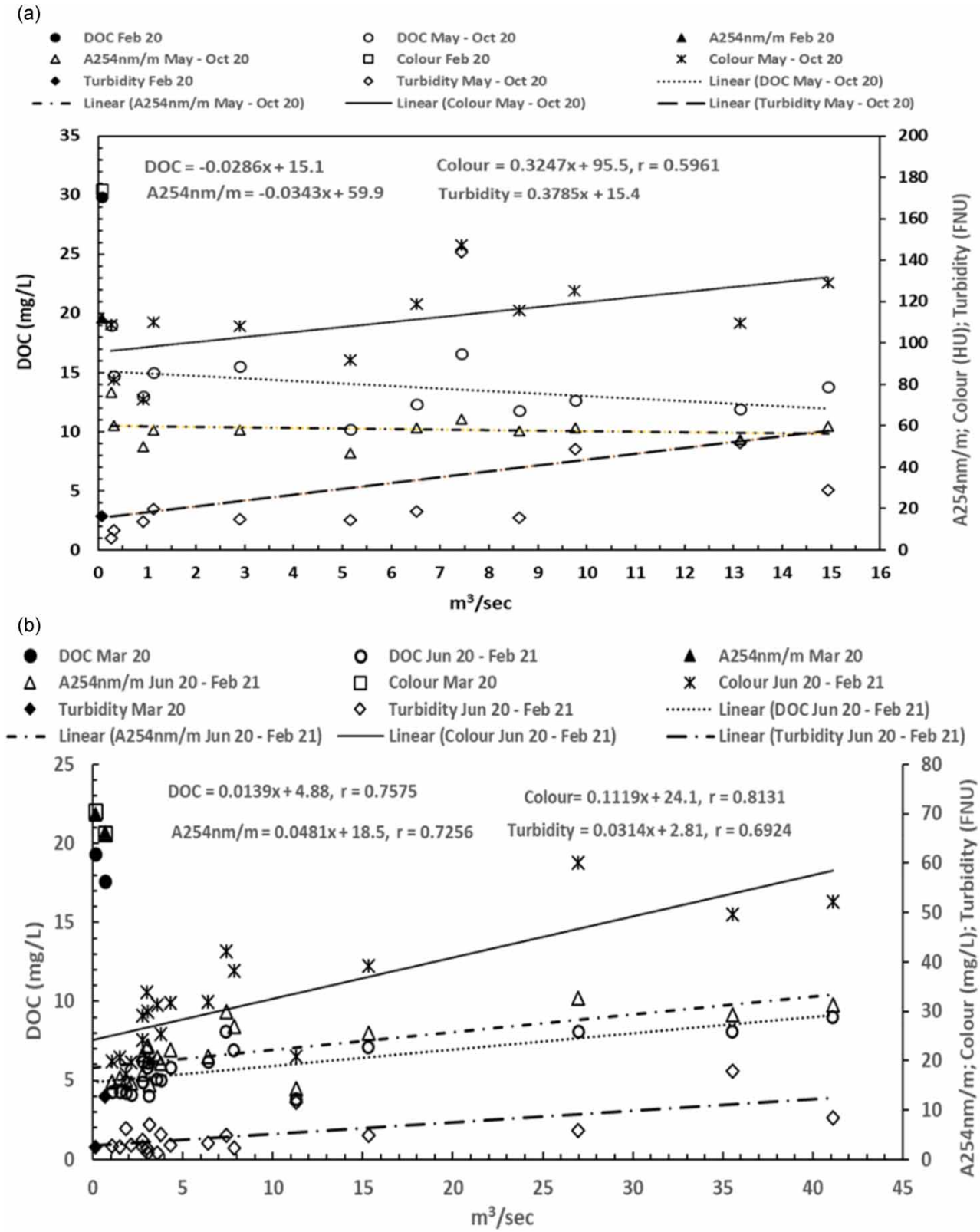

Figure 6 | Trends between daily river flows with DOC, A254 nm/m, colour, and turbidity levels for (a) the Middle River (May–October 2020) and (b) the Orroral River (June 2020–February 2021).

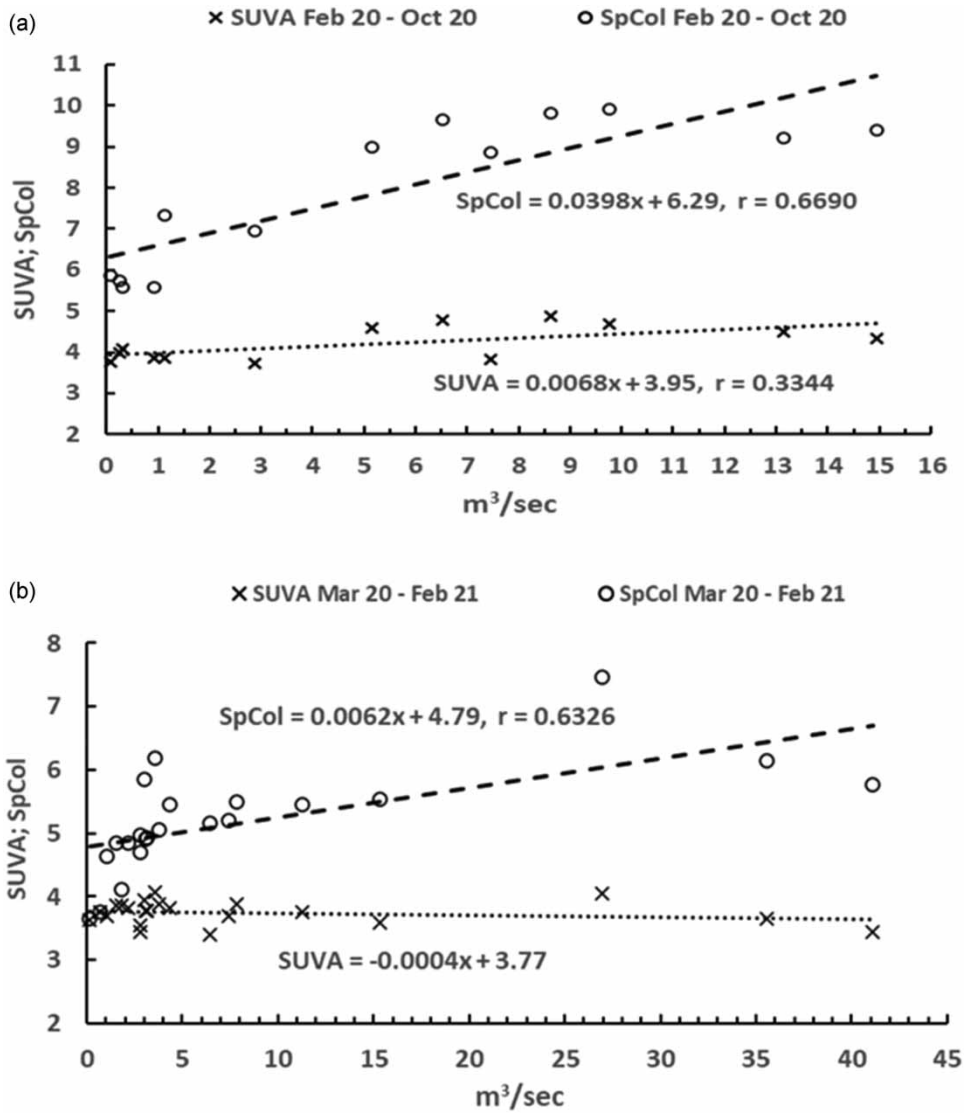

Figure 7 | Linear relationships of SUVA and SpCol with river flows (L/s) for (a) Middle River (February–October 2020) and (b) Orroral River (March 2020–February 2021).

that can rapidly provide these water quality data. Each model also has the capability to be easily adjusted for a specific water resource to align alum dose prediction to a nominally set % coagulable DOC removal, using data acquired by jar testing.

As found in this and similar studies, water quality can change rapidly and dramatically following extreme climate events that impact catchments and consequently their streams and rivers, and subsequently water resources downstream. Further changes can occur over time as the catchments restabilize dependent on vegetation regrowth, topography, soils, and land-use practices. In this study, two rivers with contrasting catchments and management, one of native vegetation of a national park and the other of mixed land management practices (dryland agriculture, silviculture, and conservation) showed different water qualities following extensive wildfires in their catchments; the highest levels of DOM and turbidities were of the catchment with mixed management practices. With predictions of more frequent occurrences of extreme climate events arising from climate change, there are also increased risks to the quality of waters from catchments impacted by such events. Hence, water treatment capabilities that enable reliable responses to rapidly changing and contrasting raw water qualities are highly important to ensure consistent supply of high-quality drinking water. The coagulant dose prediction models described and applied here are designed to encompass water qualities from such extreme climate events. These models

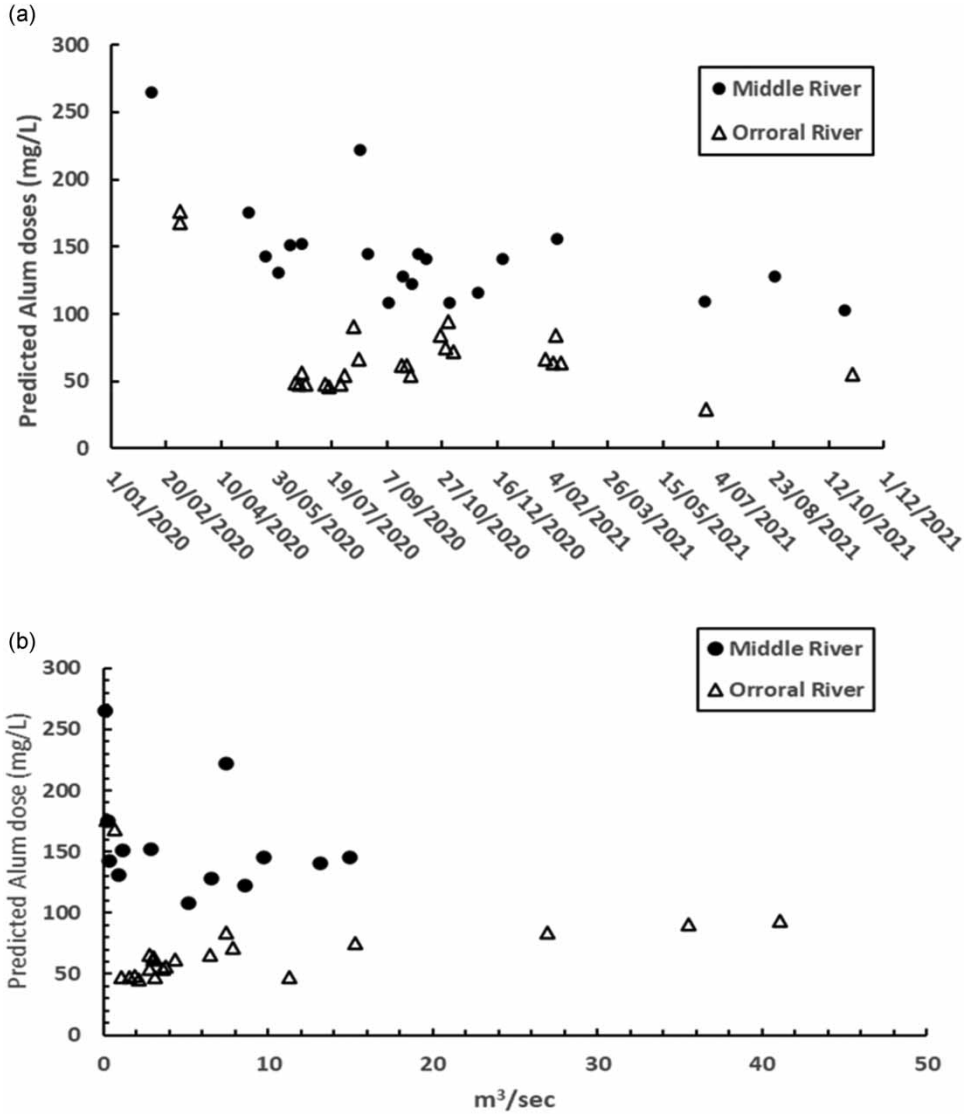

Figure 8 | Model-determined alum doses for the two surface waters post the fires (a) in the first year after the fires and (b) in comparison with river flow rates.

can be readily adjusted to account for specific raw water qualities and for meeting particular treated water quality targets. These will be further evaluated in future occurrences of extreme climate events that impact water resources.

4. CONCLUSIONS

We investigated the effects of wildfire on DOM in two contrasting river catchments: (1) Middle River (~14,500 ha), which is mixed dryland agriculture and native vegetation and (2) Orroral Valley (~9,000 ha), which is conserved as mostly intact native forest. Sentinal-2 dNBR time-series analysis of the Middle River and Orroral catchments following the 2019/2020 wildfires indicated that both catchments were burnt at high severity, although the fire severity in the Middle River catchment was more variable. After the wildfire, the Middle River catchment revegetated rapidly and subsequently showed seasonal variation due to the prominent presence of pasture grasses, while the recovery of forest vegetation in the Orroral River catchment was more gradual. Soon after the wildfires, DOC (mg/L), A254 nm/m, and colour (HU) were recorded at very high levels when river flow rates were very low. These declined to much lower levels by the end of autumn and the start of winter of the first year after the fires. However, these variations occurred at different rates at the two sites studied. The specific colour of the river waters was comparatively low soon after the wildfires, which may have been due to higher UV irradiance-induced

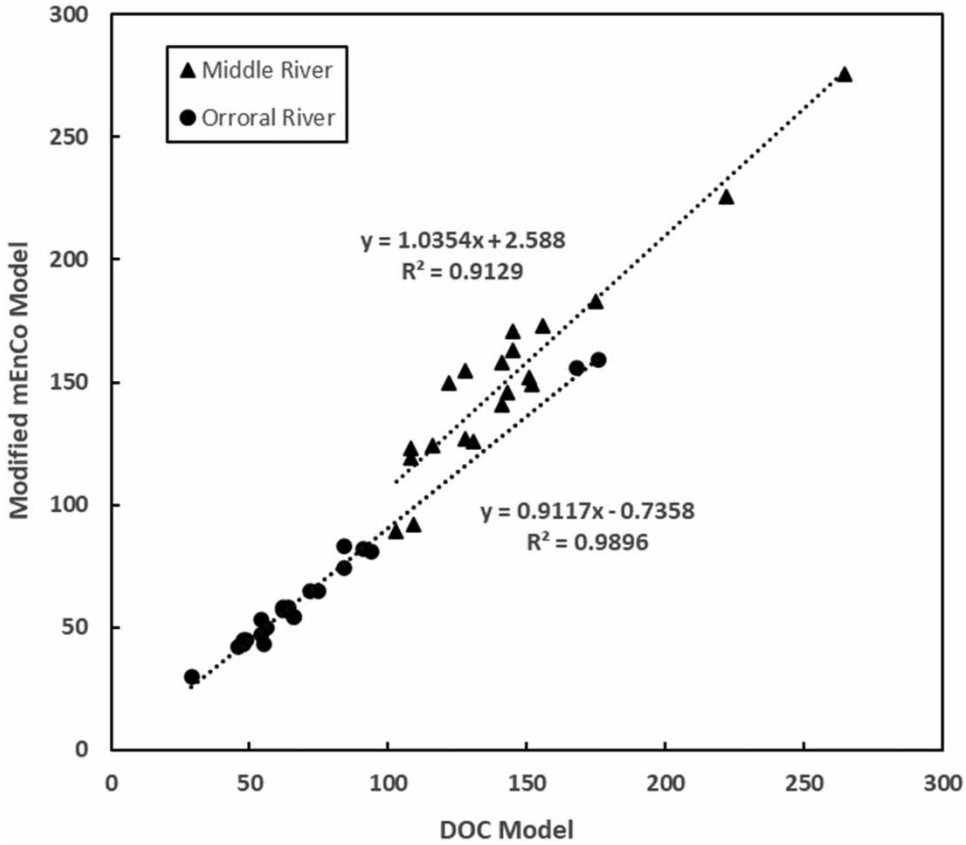

Figure 9 | Correlations between alum doses (mg/L) predicted using the DOC-based model and the modified *mEnCo* model.

cleavage of chromophoric components of DOM and higher relative abundances of organic compounds derived from algae and cyanobacteria than in the subsequently collected waters. A specific colour was also found to be related to river flow rates, while TDS concentration was found to be inversely related. The very high DOM concentrations in the river waters soon after the wildfires occurred when river flow rates were low likely contributed to by high evaporation rates caused by the wildfires and the subsequent hot summer conditions. Following catchment rainfalls and increases in river flows, DOM concentrations lowered at the sampling sites. Alum doses required in conventional treatment for drinking water supply were investigated using two prediction models that are based on different sets of input data (DOC and turbidity; UV@254 nm/cm, colour, and turbidity). The predicted doses are very high for these waters directly after the wildfires and decline to much lower levels as DOM levels become correspondingly less and when turbidity levels remain low. With the prediction of more frequent occurrences of extreme climate events resulting from climate change, such models might be of benefit in the management and treatment of source waters used for drinking water supply.

ACKNOWLEDGEMENTS

This research was supported by the Australian Government through the Australian Research Council (ARC LP160100217), SEQ Water, Melbourne Water, and Xylem Analytics Australia. The authors gratefully acknowledge Mrs Amanda Mussared, SA Water Corporation, for the provision of data on the Middle River water quality, Professor John Boland, UniSA, for advice on statistical analyses, and Professor Rodney Stewart, Griffiths University, for his advice and project support.

AUTHORS' CONTRIBUTIONS

H.D.: Methodology, Software, Investigation, Writing – Original Draft. J.A.: Conceptualization, Methodology, Writing – Review and Editing, Supervision, Formal analysis. Adam Leavesley: Investigation, Resources, Writing – Review and Editing. M.A.: Investigation, Resources, Writing – Review and Editing. E.J.: Formal analysis, Writing – Review and Editing. M.G.:

Formal analysis, Writing – Review and Editing. K.C.: Resources, Writing – Review and Editing. E.B.: Writing – Review and Editing, Supervision. J.L.: Conceptualization, Formal analysis, Writing – Review and Editing, Supervision, Project administration.

FUNDING

This research was financially supported by the Australian Government through the Australian Research Council under Grant Agreement No [ARC LP160100217].

ETHICS APPROVAL AND CONSENT TO PARTICIPATE

This research did not involve human participants, their data, or biological material. For this research, no ethical approval or consent to participate is required.

DATA AVAILABILITY STATEMENT

All relevant data are included in the paper or its Supplementary Information.

CONFLICT OF INTEREST

The authors declare there is no conflict.

REFERENCES

ACT Government (2020) Rapid Risk Assessment Team – February 2020. *Orroral Valley Fire Rapid Risk Assessment Namadgi National Park*. Unpublished Report (20/0197). Environment, Planning and Sustainable Development Directorate. Canberra: ACT Government.

Awad, J., van Leeuwen, J., Abate, D., Pichler, M., Bestland, E., Chittleborough, D. J., Fleming, N., Cohen, J., Liffner, J. & Drikas, M. (2015) The effect of vegetation and soil texture on the nature of organics in runoff from a catchment supplying water for domestic consumption, *Science of The Total Environment*, **529**, 72–81. https://doi.org/10.1016/j.scitotenv.2015.05.037.

Awad, J., van Leeuwen, J., Liffner, J., Chow, C. & Drikas, M. (2016) Treatability of organic matter derived from surface and subsurface waters of drinking water catchments, *Chemosphere*, **144**, 1193–1200. https://doi.org/10.1016/j.chemosphere.2015.09.066.

Awad, J., van Leeuwen, J., Chow, C. W. K., Smernik, R. J., Anderson, S. J. & Cox, J. W. (2017) Seasonal variation in the nature of DOM in a river and drinking water reservoir of a closed catchment, *Environmental Pollution*, **220**, 788–796. https://doi.org/10.1016/j.envpol.2016.10.054.

Bennett, L. E. & Drikas, M. (1993) The evaluation of colour in natural waters, *Water Research*, **27** (7), 1209–1218. https://doi.org/10.1016/0043-1354(93)90013-8.

Bertone, E., Sahin, O., Richards, R. & Roiko, A. (2016) Extreme events, water quality and health: A participatory Bayesian risk assessment tool for managers of reservoirs, *Journal of Cleaner Production*, **135**, 657–667. https://doi.org/10.1016/j.jclepro.2016.06.158.

Bertone, E., Sahin, O., Richards, R. & Roiko, A. (2018) Assessing the impacts of extreme weather events on potable water quality: The value to managers of a highly participatory, integrated modelling approach, *H2Open Journal*, **2** (1), 9–24. https://doi.org/10.2166/h2oj.2019.024.

Biswas, T. K., Karim, F., Kumar, A., Wilkinson, S., Guerschman, J., Rees, G., McInerney, P., Zampatti, B., Sullivan, A., Nyman, P., Sheridan, G. J. & Joehnk, K. (2021) 2019–2020 Bushfire impacts on sediment and contaminant transport following rainfall in the Upper Murray River catchment, *Integrated Environmental Assessment and Management*, **17** (6), 1203–1214. https://doi.org/10.1002/ieam.4492.

BOM (2020) *Extreme Heat and Fire Weather in December 2019 and January 2020*. Special Climate Statement 73. Australian Government Bureau of Meteorology.

Caccamo, G., Bradstock, R., Collins, L., Penman, T. & Watson, P. (2015) Using MODIS data to analyse post-fire vegetation recovery in Australian eucalypt forests, *Journal of Spatial Science*, **60** (2), 341–352. https://doi.org/10.1080/14498596.2015.974227.

Chuvieco, E., Aguado, I., Salas, J., García, M., Yebra, M. & Oliva, P. (2020) Satellite remote sensing contributions to wildland fire science and management, *Current Forestry Reports*, **6** (2), 81–96. https://doi.org/10.1007/s40725-020-00116-5.

Dalva, M. & Moore, T. R. (1991) Sources and sinks of dissolved organic carbon in a forested swamp catchment, *Biogeochemistry*, **15** (1), 1–19.

Daraei, H., Awad, J., Bertone, E., Stewart, R. A., Chow, C. W. K., Duan, J., Creamer, J. & Van Leeuwen, J. (2023a) DOC signal-based alum dose control for drinking water treatment plants, *Journal of Water Process Engineering*, **54**, 103934. https://doi.org/10.1016/j.jwpe.2023.103934.

Daraei, H., Bertone, E., Awad, J., Stewart, R. A., Chow, C. W. K., Duan, J. & Van Leeuwen, J. (2023b) A multi-analytical approach to investigate DOM dynamics and alum dose control in enhanced coagulation process using wide-ranging surface waters, *Journal of Water Process Engineering*, **56**, 104368. https://doi.org/10.1016/j.jwpe.2023.104368.

DAWE (2023) *Blackwater Events and Water Quality*. Available at: https://www.waterquality.gov.au/issues/blackwater-events (Accessed: 11 July 2023).

DCCEEW (2022) *Bushfire Recovery for Wildlife and Their Habitat: Kangaroo Island*. Available at: https://www.dcceew.gov.au/environment/biodiversity/bushfire-recovery/regional-delivery-program/kangaroo-island#:~:text=The%20Australian%20Government%20is%20investing,ecological%20communities%20and%20natural%20assets (Accessed: 08 March 2024).

DEWNR (2013) *Non-prescribed Surface Water Resources Assessment Kangaroo Island Natural Resources Management Region*. Department of Environment, Water and Natural Resources.

Edzwald, J. K. & Tobiason, J. E. (1999) Enhanced coagulation: US requirements and a broader view, *Water Science and Technology*, **40** (9), 63–70. https://doi.org/10.1016/S0273-1223(99)00641-1.

Escuin, S., Navarro, R. & Fernández, P. (2008) Fire severity assessment by using NBR (normalized burn ratio) and NDVI (normalized difference vegetation index) derived from LANDSAT TM/ETM images, *International Journal of Remote Sensing*, **29** (4), 1053–1073. https://doi.org/10.1080/01431160701281072.

Fornacca, D., Ren, G. & Xiao, W. (2018) Evaluating the best spectral indices for the detection of burn scars at several post-fire dates in a mountainous region of northwest Yunnan, China, *Remote Sensing*, **10** (8), 1196.

Gale, M. G., Cary, G. J., Yebra, M., Leavesley, A. J. & Van Dijk, A. I. J. M. (2022) Comparison of contrasting optical and LiDAR fire severity remote sensing methods in a heterogeneous forested landscape in south-eastern Australia, *International Journal of Remote Sensing*, **43** (7), 2538–2559. https://doi.org/10.1080/01431161.2022.2064197.

Gibson, R. K. & Hislop, S. (2022) Signs of resilience in resprouting eucalyptus forests, but areas of concern: 1 year of post-fire recovery from Australia's black summer of 2019–2020, *International Journal of Wildland Fire*, **31** (5), 545–557.

Golea, D. M., Upton, A., Jarvis, P., Moore, G., Sutherland, S., Parsons, S. A. & Judd, S. J. (2017) THM and HAA formation from NOM in raw and treated surface waters, *Water Research*, **112**, 226–235. https://doi.org/10.1016/j.watres.2017.01.051.

Hogue, T. S. & McCray, J. (2018) *Post-Fire Water Quality: An Investigation of Determinants and Recovery Processes in Burned Watersheds across the Western US, October 1, 2014–September 30, 2018*. USGS. Available at: firescience.gov.

Huang, W., McDowell, W. H., Zou, X., Ruan, H., Wang, J. & Ma, Z. (2015) Qualitative differences in headwater stream dissolved organic matter and riparian water-extractable soil organic matter under four different vegetation types along an altitudinal gradient in the Wuyi Mountains of China, *Applied Geochemistry*, **52**, 67–75. https://doi.org/10.1016/j.apgeochem.2014.11.014.

Huff, D. K., Morris, L. A., Sutter, L., Costanza, J. & Pennell, K. D. (2020) Accumulation of six PFAS compounds by woody and herbaceous plants: Potential for phytoextraction, *International Journal of Phytoremediation*, **22** (14), 1538–1550. https://doi.org/10.1080/15226514.2020.1786004.

Johnston, S. G. & Maher, D. T. (2022) Drought, megafires and flood – Climate extreme impacts on catchment-scale river water quality on Australia's east coast, *Water Research*, **218**, 118510. https://doi.org/10.1016/j.watres.2022.118510.

Kaiser, K. & Zech, W. (1997) Competitive sorption of dissolved organic matter fractions to soils and related mineral phases, *Soil Science Society of America Journal*, **61** (1), 64–69. https://doi.org/10.2136/sssaj1997.03615995006100010011x.

Ke, Y., Calmels, D., Bouchez, J. & Quantin, C. (2022) MOdern river archivEs of particulate organic carbon: MOREPOC, *Earth System Science Data*, **14** (10), 4743–4755. https://doi.org/10.5194/essd-14-4743-2022.

Key, C. H. & Benson, N. C. (2006) Landscape assessment: Ground measure of severity, the composite burn index; and the remote sensing of severity, the normalized burn ratio. FIREMON: Fire effects monitoring and inventory system. RMRS-GTR-164. Publisher: USDA Forest Service, Rocky Mountain Research Station, Ogden, UT; Editors: D.C. Lutes, R.E. Keane, J.F. Caratti, C.H. Key, N.C. Benson, S. Sutherland, L.J. Gangi.

Krause, C., Dunn, B., Bishop-Taylor, R., Adams, C., Burton, C., Alger, M., Chua, S., Phillips, C., Newey, V., Kouzoubov, K. & Leith, A. (2021) Digital Earth Australia notebooks and tools repository. Geoscience Australia) Available at https://docs. dea. ga. gov. au/notebooks/README. html.

Kreutzweiser, D. P. & Capell, S. S. (2003) Benthic microbial utilization of differential dissolved organic matter sources in a forest headwater stream, *Canadian Journal of Forest Research*, **33** (8), 1444–1451. https://doi.org/10.1139/x03-030.

Lewis, A., Oliver, S., Lymburner, L., Evans, B., Wyborn, L., Mueller, N., Raevksi, G., Hooke, J., Woodcock, R., Sixsmith, J., Wu, W., Tan, P., Li, F., Killough, B., Minchin, S., Roberts, D., Ayers, D., Bala, B., Dwyer, J., Dekker, A., Dhu, T., Hicks, A., Ip, A., Purss, M., Richards, C., Sagar, S., Trenham, C., Wang, P. & Wang, L.-W. (2017) The Australian geoscience data cube – Foundations and lessons learned, *Remote Sensing of Environment*, **202**, 276–292. https://doi.org/10.1016/j.rse.2017.03.015.

Li, F., Jupp, D. L. B., Reddy, S., Lymburner, L., Mueller, N., Tan, P. & Islam, A. (2010) An evaluation of the use of atmospheric and BRDF correction to standardize Landsat data, *IEEE Journal of Selected Topics in Applied Earth Observations and Remote Sensing*, **3** (3), 257–270. https://doi.org/10.1109/JSTARS.2010.2042281.

Li, F., Jupp, D. L. B., Thankappan, M., Lymburner, L., Mueller, N., Lewis, A. & Held, A. (2012) A physics-based atmospheric and BRDF correction for Landsat data over mountainous terrain, *Remote Sensing of Environment*, **124**, 756–770. https://doi.org/10.1016/j.rse.2012.06.018.

Lu, B., He, Y. & Tong, A. (2016) Evaluation of spectral indices for estimating burn severity in semiarid grasslands, *International Journal of Wildland Fire*, **25** (2), 147–157. https://doi.org/10.1071/WF15098.

Mannik, R. D., Herron, A., Hill, P. I., Brown, R. E. & Moran, R. (2013) Estimating the change in streamflow resulting from the 2003 and 2006/2007 bushfires in southeastern Australia, *Australasian Journal of Water Resources*, **16** (2), 107–120. https://doi.org/10.7158/13241583.2013.11465408.

Mansilha, C., Duarte, C. G., Melo, A., Ribeiro, J., Flores, D. & Marques, J. E. (2019) Impact of wildfire on water quality in Caramulo Mountain ridge (Central Portugal), *Sustainable Water Resources Management*, **5** (1), 319–331. https://doi.org/10.1007/s40899-017-0171-y.

Miller, J. D. & Thode, A. E. (2007) Quantifying burn severity in a heterogeneous landscape with a relative version of the delta normalized burn ratio (dNBR), *Remote Sensing of Environment*, **109** (1), 66–80. https://doi.org/10.1016/j.rse.2006.12.006.

Mosley, L. M., Wallace, T., Rahman, J., Roberts, T. & Gibbs, M. (2021) An integrated model to predict and prevent hypoxia in floodplain-river systems, *Journal of Environmental Management*, **286**, 112213. https://doi.org/10.1016/j.jenvman.2021.112213.

Massetti, A., Rüdiger, C., Yebra, M. & Hilton, J. (2019) The Vegetation Structure Perpendicular Index (VSPI): A forest condition index for wildfire predictions. Remote Sensing of Environment, 224, pp. 167–181.

Mostofa, K. M., Yoshioka, T., Mottaleb, A. & Vione, D. (2013) *Photobiogeochemistry of Organic Matter: Principles and Practices in Water Environments*. Springer Heidelberg New York Dordrecht London: Springer Science & Business Media. https://doi.org/10.1007/978-3-642-32223-5.

Murshed, M. F., Aslam, Z., Lewis, R., Chow, C., Wang, D., Drikas, M. & van Leeuwen, J. (2014) Changes in the quality of river water before, during and after a major flood event associated with a La Niña cycle and treatment for drinking purposes, *Journal of Environmental Science (China)*, **26** (10), 1985–1993. https://doi.org/10.1016/j.jes.2014.08.001.

Neris, J., Santin, C., Lew, R., Robichaud, P. R., Elliot, W. J., Lewis, S. A., Sheridan, G., Rohlfs, A.-M., Ollivier, Q., Oliveira, L. & Doerr, S. H. (2021) Designing tools to predict and mitigate impacts on water quality following the Australian 2019/2020 wildfires: Insights from Sydney's largest water supply catchment, *Integrated Environmental Assessment and Management*, **17** (6), 1151–1161. https://doi.org/10.1002/ieam.4406.

Niquette, P., Servais, P. & Savoir, R. (2001) Bacterial dynamics in the drinking water distribution system of Brussels, *Water Research*, **35** (3), 675–682. https://doi.org/10.1016/s0043-1354(00)00303-1.

Nolan, R. H., Bowman, D. M., Clarke, H., Haynes, K., Ooi, M. K., Price, O. F., Williamson, G. J., Whittaker, J., Bedward, M. & Boer, M. M. (2021) What do the Australian black summer fires signify for the global fire crisis? *Fire*, **4** (4), 97.

Quill, E. S., Angove, M. J., Morton, D. W. & Johnson, B. B. (2010) Characterisation of dissolved organic matter in water extracts of thermally altered plant species found in box–ironbark forests, *Soil Research*, **48** (8), 693–704. https://doi.org/10.1071/SR09157.

Richards, L., Brew, N. & Smith, L. (2020) *20 Australian Bushfires – Frequently Asked Questions: A Quick Guide*. Research Paper Series, 2019–20. Department of Parliamentary Services, Parliament of Australia.

Sachse, A., Henrion, R., Gelbrecht, J. & Steinberg, C. E. W. (2005) Classification of dissolved organic carbon (DOC) in river systems: Influence of catchment characteristics and autochthonous processes, *Organic Geochemistry*, **36** (6), 923–935. https://doi.org/10.1016/j.orggeochem.2004.12.008.

Sherson, L. R., Van Horn, D. J., Gomez-Velez, J. D., Crossey, L. J. & Dahm, C. N. (2015) Nutrient dynamics in an alpine headwater stream: Use of continuous water quality sensors to examine responses to wildfire and precipitation events, *Hydrological Processes*, **29** (14), 3193–3207. https://doi.org/10.1002/hyp.10426.

Teksoy, A., Alkan, U. & Başkaya, H. S. (2008) Influence of the treatment process combinations on the formation of THM species in water, *Separation and Purification Technology*, **61** (3), 447–454. https://doi.org/10.1016/j.seppur.2007.12.008.

van Leeuwen, J., Page, D., Spark, K., Fabris, R. & Sledz, L. (2023) Characterisation of Natural Organic Matter in Relation to Drinking Water and Alum Treatment. Cooperative Research Centre for Water Quality and Treatment, Australian Water Quality Centre, Adelaide, South Australia. Report No. 15, August 2001. ISBN 1878818172.

van Leeuwen, J., Daly, R. & Holmes, M. (2005) Modeling the treatment of drinking water to maximize dissolved organic matter removal and minimize disinfection by-product formation, *Desalination*, **176** (1), 81–89. https://doi.org/10.1016/j.desal.2004.10.024.

van Leeuwen, J., Holmes, M., Kaeding, U., Daly, R. & Bursill, D. (2009) Development and implementation of the software mEnCo© to predict coagulant doses for DOC removal at full-scale WTPs in South Australia, *Journal of Water Supply: Research and Technology-Aqua*, **58** (4), 291–298. https://doi.org/10.2166/aqua.2009.054.

van Oldenborgh, G. J., Krikken, F., Lewis, S., Leach, N. J., Lehner, F., Saunders, K. R., van Weele, M., Haustein, K., Li, S., Wallom, D., Sparrow, S., Arrighi, J., Singh, R. K., van Aalst, M. K., Philip, S. Y., Vautard, R. & Otto, F. E. L. (2021) Attribution of the Australian bushfire risk to anthropogenic climate change, *Natural Hazards and Earth System Sciences*, **21** (3), 941–960. https://doi.org/10.5194/nhess-21-941-2021.

Wang, D., Zhao, Y., Xie, J., Chow, C. W. K. & van Leeuwen, J. (2013) Characterizing DOM and removal by enhanced coagulation: A survey with typical Chinese source waters, *Separation and Purification Technology*, **110**, 188–195. https://doi.org/10.1016/j.seppur.2013.03.020.

Young, K. C., Docherty, K. M., Maurice, P. A. & Bridgham, S. D. (2005) Degradation of surface-water dissolved organic matter: Influences of DOM chemical characteristics and microbial populations, *Hydrobiologia*, **539** (1), 1–11. https://doi.org/10.1007/s10750-004-3079-0.

First received 2 April 2024; accepted in revised form 11 September 2024. Available online 1 October 2024